

See discussions, stats, and author profiles for this publication at: <https://www.researchgate.net/publication/230669613>

# Gas-Sensitive Photoconductivity of Porphyrin-Functionalized ZnO Nanorods

ARTICLE *in* THE JOURNAL OF PHYSICAL CHEMISTRY C · APRIL 2012

Impact Factor: 4.77 · DOI: 10.1021/jp302225u

---

CITATIONS

29

READS

152

## 8 AUTHORS, INCLUDING:



Alexandro Catini

University of Rome Tor Vergata

41 PUBLICATIONS 150 CITATIONS

[SEE PROFILE](#)



Gabriele Magna

32 PUBLICATIONS 80 CITATIONS

[SEE PROFILE](#)



Francesco Basoli

Università Campus Bio-Medico di Roma

25 PUBLICATIONS 82 CITATIONS

[SEE PROFILE](#)



Roberto Paolesse

University of Rome Tor Vergata

422 PUBLICATIONS 6,772 CITATIONS

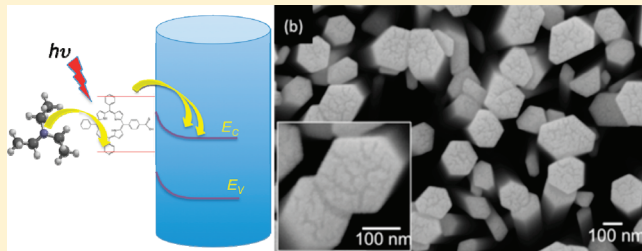
[SEE PROFILE](#)

# Gas-Sensitive Photoconductivity of Porphyrin-Functionalized ZnO Nanorods

Yuvaraj Sivalingam,<sup>†</sup> Eugenio Martinelli,<sup>†</sup> Alessandro Catini,<sup>†</sup> Gabriele Magna,<sup>†</sup> Giuseppe Pomarico,<sup>‡</sup> Francesco Basoli,<sup>‡</sup> Roberto Paolesse,<sup>‡</sup> and Corrado Di Natale<sup>\*,†</sup>

<sup>†</sup>Department of Electronic Engineering and <sup>‡</sup>Department of Chemical Science and Technology, University of Rome Tor Vergata, 00133 Roma, Italy

**ABSTRACT:** Hybrid materials based on wide band gap semiconductors and dye molecules are intensively studied for photovoltaic applications. However, these materials also possess interesting gas sensitivities, besides these photonic effects. In this Article, we report the study, under visible light illumination, of the porphyrin-functionalized ZnO nanorod photoconductivity changes, modulated by exposure to two volatile organic compounds, ethanol and triethylamine, chosen as model analytes. The sensitivity to triethylamine exceeds that to ethanol by more than two orders of magnitude, showing a selectivity that is not found in other porphyrin-based gas sensors. This feature could open the way to a novel generation of sensors, where photoactivation plays a role in determining both sensitivity and selectivity of the resulting device.



## INTRODUCTION

Hybrid materials formed by a layer of dye molecules attached to a wide-band gap semiconductor are nowadays a hot research topic because they are the key component of dye-sensitized solar cells.<sup>1</sup> However the combination of these two materials can offer other additional properties, besides the conversion of visible photons into an excess of carriers. One important characteristic, for example, is the gas sensing; metal oxide semiconductors are in fact among the most diffused materials for chemical sensors, and several dye molecules have brilliant capabilities to bind airborne compounds.

ZnO and porphyrins are, respectively, good examples of a metal oxide semiconductor and a dye molecule. ZnO is a wide band gap (3.37 eV) semiconductor with large exciton binding energy (60 meV). It has been studied for gas sensors,<sup>2</sup> optoelectronics and electronic devices,<sup>3,4</sup> photoanodes for dye sensitized solar cells,<sup>5</sup> and mechanical energy harvesting.<sup>6</sup> So far, numerous ZnO nanostructures with different sizes and morphologies have been synthesized, such as nanowires, nanorods, and nanotubes.<sup>7</sup>

Porphyrins are among the most versatile ligand platform, forming a wide range of metal complexes; they can interact with airborne molecules by a large spectrum of different mechanisms. The large  $\pi$ -electron system allows porphyrins to act as both electron donors and acceptors. This capability has been exploited to develop chemical sensors mostly based on quartz microbalances<sup>8,9</sup> and optical transducers.<sup>10,11</sup> Usually porphyrin-based gas sensors are scarcely selective; consequently, their large versatility of interactions is fully exploited in sensor array configurations.<sup>12</sup>

The ligand flexibility of porphyrins makes them suitable to form hybrid materials, where the richness of porphyrin binding

interactions strongly contributes and enriches the overall gas sensing. For instance, gas sensors formed by porphyrin-coated carbon nanotube bundles have been demonstrated.<sup>13</sup> This approach was also used with metal oxide semiconductors, such as ZnO and SnO<sub>2</sub>, and in this case the addition of a porphyrin layer to the surface of metal-oxide semiconductors strongly reduces the sensor operating temperature, making possible the detection of volatile organic compounds (VOCs) at temperature of  $\sim 100$  °C.<sup>14,15</sup>

The cooperation of porphyrins and ZnO gives rise to hybrid structures whose properties may exceed those of the individual constituents. For instance the enhancement of photovoltaic properties was observed in porphyrin-functionalized ZnO nanorods.<sup>16</sup> The photonic effects in these structures can also lead to an improved catalytic efficiency,<sup>17</sup> which has been recently exploited for the solution detection of cysteine by porphyrin-functionalized ZnO nanoparticles.<sup>18</sup>

All of these results indicate that light may also interfere with the binding of guest molecules onto the porphyrin–ZnO complex. To explore this conjecture, we developed a gas sensor device formed by an array of ZnO nanorods, coated with a layer of a tetraphenylporphyrin bearing a peripheral carboxylic group (Figure 1) to favor the anchoring onto the ZnO surface.<sup>19,20</sup> The device demonstrates that the contemporaneous sensitivity to light and gas gives place to a photoconductive gas sensor. The sensing mechanism involves an initial charge transfer from the adsorbed molecule to the porphyrin and then the photoinduced transfer of the charge from the porphyrin to

Received: March 7, 2012

Revised: March 30, 2012

Published: April 3, 2012

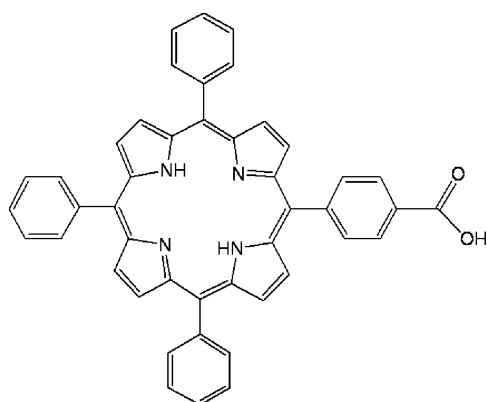


**Figure 1.** Molecular structure of the 5-(4'-carboxyphenyl)-10,15,20-triphenylporphyrin (H<sub>2</sub>TPPCOOH).

the semiconductor. Eventually, a change of the resistance of the device is observed.

## ■ EXPERIMENTAL SECTION

Reagents and solvents (Sigma-Aldrich, Fluka, and Carlo Erba Reagenti) for synthesis and purification were of synthetic grade and used as received. 5-(4'-Carboxyphenyl)-10,15,20-triphenylporphyrin (H<sub>2</sub>TPPCOOH, Figure 1) was prepared as previously reported.<sup>21</sup>

The concept of the sensor and the fabrication steps is illustrated in Figure 2. The substrate was a 300 Å ITO layer of glass with a surface resistivity of 30–60 Ω/sq (Sigma-Aldrich). A strip of the indium tin oxide (ITO) layer was removed, leaving a gap of ~200 μm between the two parts. ZnO nanorods were grown via hydrothermal route<sup>22</sup> from a seed

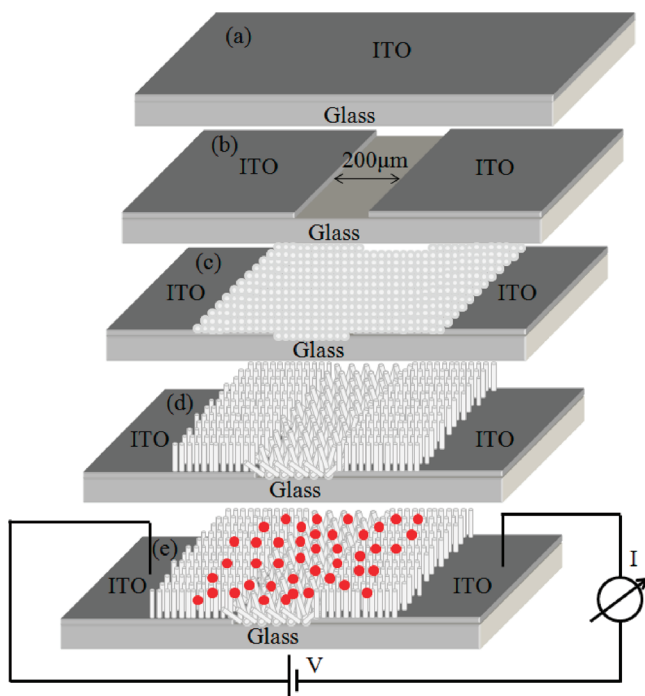


**Figure 2.** Fabrication process of the porphyrin-functionalized ZnO nanorods sensor: (a) ITO substrate on glass, (b) removal of a conductive strip and electrodes formation, (c) seed layer deposition, (d) ZnO nanorods growth, and (e) porphyrins coating.

layer deposited with a drop coating method in the gap and on the rims of the ITO layer.

The ZnO seed layer solution was prepared by adding zinc acetate (54.9 mg) to 50 mL of absolute ethanol. To enhance the wetting of the seed layer on ITO substrates, we irradiated the substrates by UV lamp for 20 min. The formation of the seed layer on ITO substrate was conducted by using drop-coating method. After ZnO seed layer coating on the ITO substrates, the substrates were post-annealed in air at 400 °C for 30 min. ITO substrates with seed layer were then vertically inserted into 200 mL of the aqueous precursor solution (0.025 mol/L of zinc acetate dihydrate and hexamethyltetramine) to allow the growth of ZnO nanorods at 90 °C for 4 h. After nanorod growth, the substrate was removed from the solution, followed by rinsing with deionized water, and then dried in air. The length of ZnO nanorods was controlled by the number of repetitive reactions and time. SEM (Cambridge 360 Microscope LaB<sub>6</sub>) was employed to characterize the nanostructure morphology.

The synthesized ZnO nanorods were functionalized by casting deposition of H<sub>2</sub>TPPCOOH 10<sup>-3</sup> mol/L in methanol solution. The coated nanorods were allowed to dry at room temperature around 1 h, and, after treatment with the H<sub>2</sub>TPPCOOH solution, the ZnO nanorod surface color turned from white to light brown. A UV-vis spectrophotometer (Varian Cary 500) and a fiber optic spectrophotometer (USB4000 miniature) were used to characterize the optical properties of uncoated and porphyrin-functionalized ZnO nanorods. *I*–*V* measurements were conducted in a closed chamber under different illuminations using a dual channel source meter (Keithley 2612). Photocurrent spectroscopy was measured by an assembled system equipped with a 100 W xenon lamp (Newport model 60000), 1/8 m monochromator (Spectral products model CM110) and a calibrated photodiode (Newport model 818-UV-L).

The response to gases was evaluated by measuring the resistance, using the same setup described for *I*–*V* measurement. The substrate with coated and uncoated ZnO nanorods was enclosed in a sealed cell endowed with a gastight optical window, suitable for both UV and visible-light illumination. Saturated vapors of ethanol and triethylamine were obtained by N<sub>2</sub> bubbling in liquid samples; then, different concentrations of these volatiles were obtained by dilution with synthetic air, used also as reference gas during the measurements. The flow at the cell inlet was kept constant at 100 mL/min by a mass flow controller (MKS). During the measurements, the liquid samples of ethanol and triethylamine were kept at a controlled temperature of 30 °C.

## ■ RESULTS AND DISCUSSION

The morphology of uncoated and porphyrin-coated ZnO nanorods is showed in the SEM images reported in Figure 3. The pristine ZnO nanorods grew vertically aligned on ITO (Figure 3a), and the H<sub>2</sub>TPPCOOH layer (Figure 3b,c) coated the nanorods along both the walls and the hexagonal face-cut section. Porphyrins appear clustered in structures of tens of nanometers size. Such a morphology suggests that the first layer of porphyrins linked to the ZnO surface promotes the successive aggregations of further macrocycles, driven by π–π interactions between porphyrin units.

Figure 3d shows an SEM image of the porphyrin-coated nanorods in the gap region. Because of the unaligned seeds, ZnO nanorods formed an interconnected network because

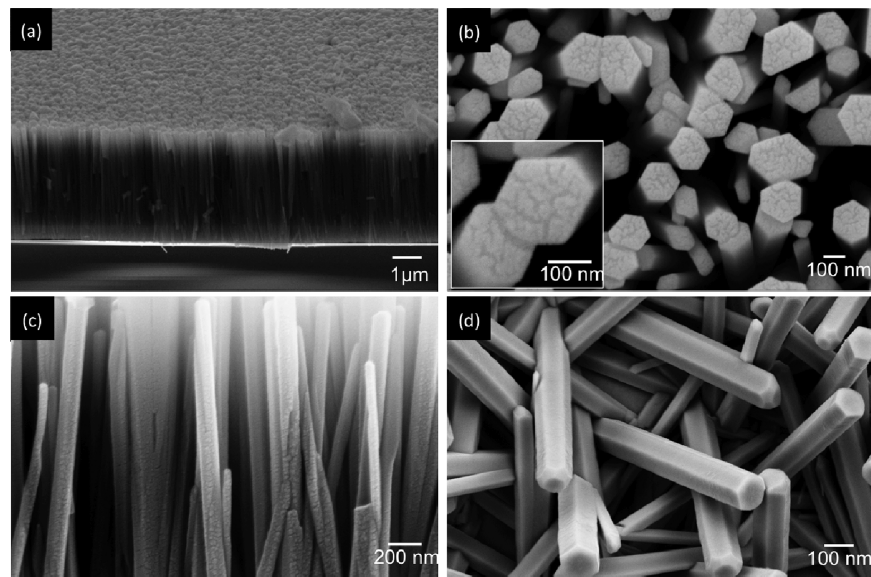


**Figure 3.** SEM images of the sensor surface. (a)  $45^\circ$  tilted view of uncoated ZnO nanorods grown on the flat ITO surface. (b) Top view of porphyrin-coated nanorods. (c) Lateral view of porphyrins coated nanorods. (d) Top view of coated ZnO nanorods in the gap region between the ITO electrodes.

under the hydrothermal conditions the side-crystal planes were able to merge together to form long crystal structures connecting the two ITO electrodes. This result evidences that the growth of long ZnO nanorods is versatile enough to allow for the formation of a continuous crystal network between the two electrodes.<sup>23</sup> The ZnO nanorods appearance is compatible with a wurtzite structure grown along the *c*-axis direction. SEM images indicate that these nanorods had a diameter of 50–100 nm and a length of 2 to 3  $\mu\text{m}$  in the gap region.

An insight into the interaction between porphyrins and ZnO can be obtained by the optical absorbance spectra. In Figure 4, the absorption spectra of ZnO nanorods, H<sub>2</sub>TPPCOOH-coated ZnO nanorods, and H<sub>2</sub>TPPCOOH in solution are

compared. The absorbance spectrum of uncoated ZnO nanorods shows a peak at 384 nm, whose tail extends into the visible range. H<sub>2</sub>TPPCOOH in solution shows the typical Soret band at 418 nm and the less intense Q-bands between 500 and 600 nm. The absorbance spectra of H<sub>2</sub>TPPCOOH-coated ZnO nanorods show a slight alteration of the peak in the UV region. In the visible region, it is possible to observe the porphyrin Soret band peak at 440 nm, characterized by a significant line broadening and red shift with respect to the solution phase absorption. Both of these spectral features are in good agreement with the porphyrin aggregation observed in Figure 3b,c.

The photoconductive features have been explored by the spectral photocurrent shown in Figure 5a. The photocurrent nicely reproduces the spectral absorbance shown in Figure 4, and it is interesting to note that the photoconductive effects observed in the visible region can be almost totally attributed to the photoinjection of electrons in the ZnO conduction band operated by the excited porphyrin layer. Following this result, H<sub>2</sub>TPPCOOH-coated ZnO nanorods were exposed to a white light LED and to a UV lamp, and Figure 5b shows the emission spectra of both light sources. A comparison of Figure 5a,b indicates that the exposure to the LED light is expected to elicit the porphyrin photoresponse, whereas the illumination with the UV lamp prompts the ZnO contribution to the photoconductivity.

The effects of the illumination in terms of the resistance of the device are shown in Figure 5c. The *I*–*V* curves have been measured with a bias voltage in the interval from −1 to +1 V. Figure 5c reports the *I*–*V* curve of uncoated and coated ZnO nanorods under different illumination conditions. As expected for a ITO-ZnO junction,<sup>24</sup> the ZnO layer is characterized by an ohmic behavior, with a dark resistance of 4100 k $\Omega$  approximately. It is straightforward that because of the wide semiconductor band gap, the resistance drops several orders of magnitude under UV illumination, whereas, as expected, the conductivity is unaffected under visible light. The dark resistance of the porphyrin coated nanorods is  $\sim$ 810 k $\Omega$ ,

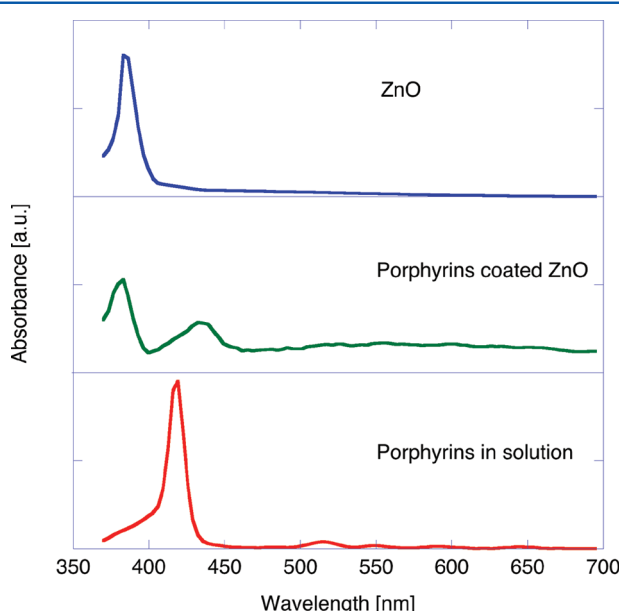


**Figure 4.** Absorbance spectra of uncoated ZnO, porphyrin-coated ZnO, and porphyrin (CHCl<sub>3</sub> solution).

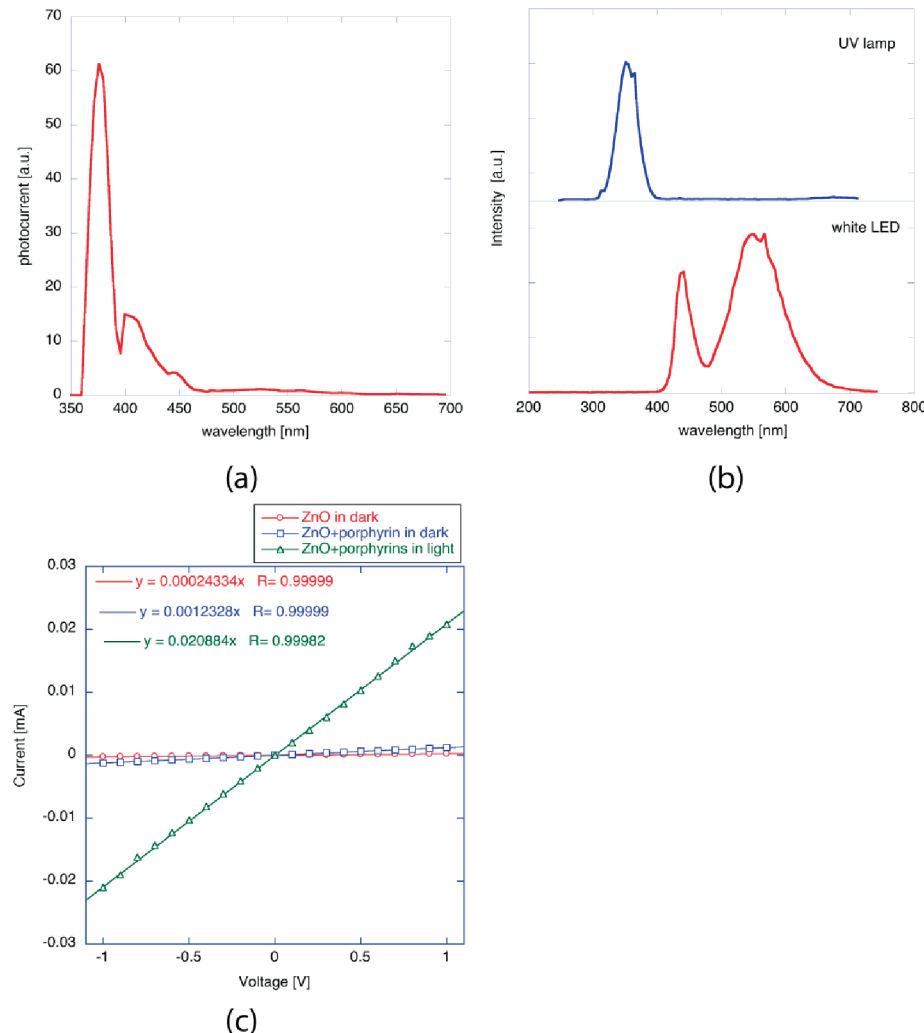


**Figure 5.** Electrical properties of the sensor. (a) Spectral photocurrent. (b) Spectral intensity of the light sources used to excite the photoconductivity. Intensity is in arbitrary units. (c)  $I$ – $V$  curves of uncoated and coated ZnO nanorods under dark and white light illumination. Linear fits are also shown. The angular coefficient of the regression equation is the conductance of the device in mS units.

which is about five times smaller than the dark resistance of the uncoated ZnO.

To understand the consequences on the ZnO conductivity of the interaction between porphyrin and ZnO, it is necessary to consider the presence of the carboxylic group that has been reported to corrode ZnO.<sup>25,26</sup> For this scope, the resistance of benzoic-acid-coated ZnO nanorods was also measured, and, as supposed, a small resistance increase was observed. As a consequence, the change of the resistance in the dark has to be attributed to the adsorbed porphyrins. The behavior observed in different organic–inorganic interfaces<sup>27</sup> suggests that the increase in conductivity may be due to the interaction of porphyrins with the surface states of ZnO, which slightly increases the density of electrons in the conduction band of the semiconductor.

The conductivity is considerably increased under white light LED illumination. Under this condition, the resistance is  $\sim 50$  k $\Omega$ , indicating an appreciable injection of photoexcited electrons from the porphyrin LUMO level to the ZnO conduction band.

To study the gas sensitivity, we have exposed the device to diluted vapors of ethanol and triethylamine. These compounds have been chosen as model analytes because they show a

different behavior as electron donors. The sensitivity of porphyrins to triethylamine and ethanol has already been demonstrated by mass, optical, and surface potential transducers.<sup>28</sup> The binding of triethylamine to a free base porphyrin, such as H<sub>2</sub>TPPCOOH, could be ascribed to a combination of van der Waals and basic hydrogen bond acceptor interactions. Porphyrins are also able to bind ethanol, where the hydrogen bond donor interaction could be considered to be the main interaction mechanism, with less intense van der Waals interactions. These molecular interaction properties can be derived from sorption models, such as linear sorption energy relationship (LSER), which provides values of the molecular interaction strength.<sup>29</sup> LSER was demonstrated in the past to provide a valid support to describe the adsorption of volatile compounds in porphyrin layers.<sup>30</sup>

For this experiment, the sensor was enclosed in a chamber endowed with gas inlet and outlet. Saturated vapors of triethylamine and ethanol were diluted in a carrier of synthetic air. The sensor was tested at three dilution factors (8, 16, and 24%), kept constant by mass flow controllers, at room temperature, where the saturated vapor pressures of ethanol and triethylamine are 5.95 and 6.89 kPa, respectively.

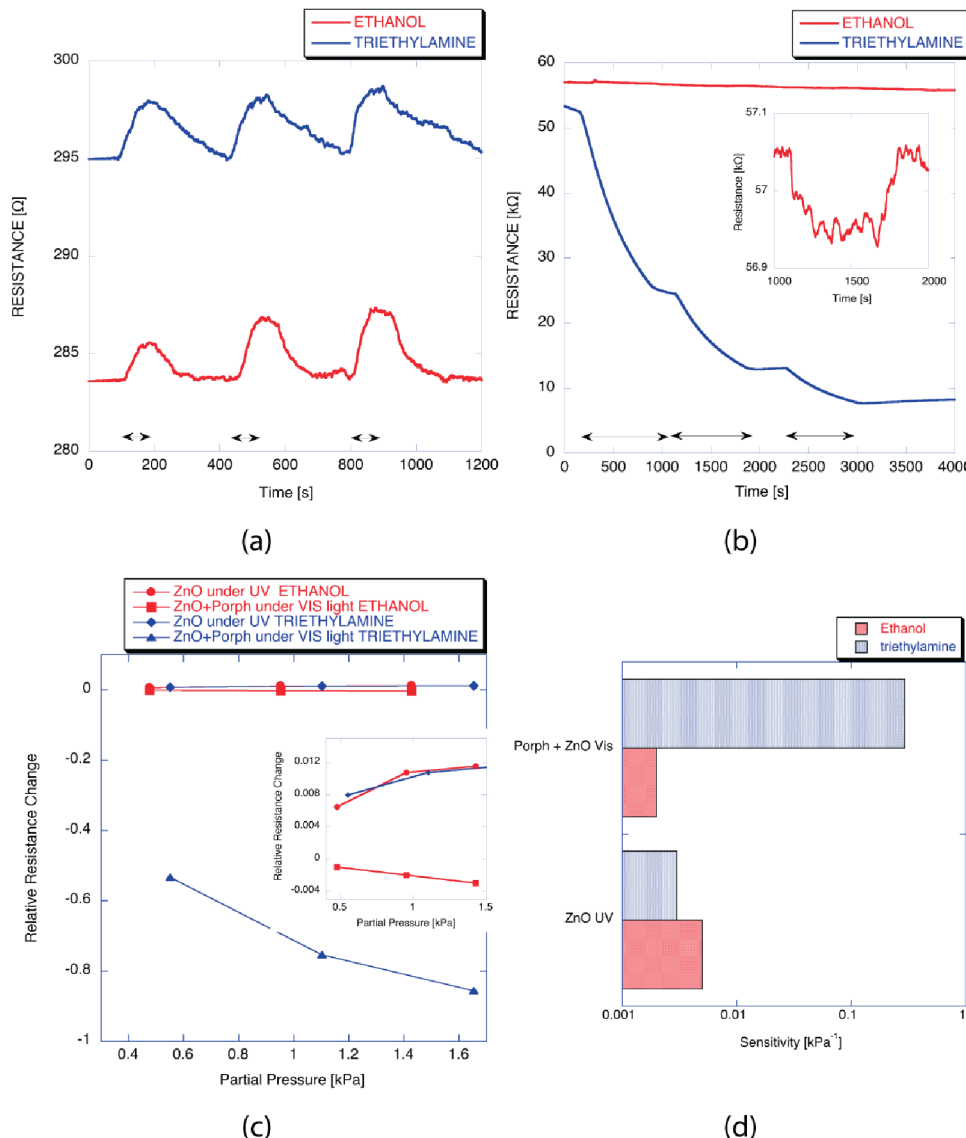


**Figure 6.** Behavior of the resistance measured during the exposure to growing concentrations of 8, 16, and 24% of saturated vapor pressure of ethanol and triethylamine diluted in synthetic air. Arrows indicate the exposure time. (a) Uncoated ZnO nanorods under UV lamp illumination. (b) Coated ZnO nanorods under white light. In the inset, the resistance during the second exposure to ethanol is shown. (c) The response curve plots of the relative resistance change calculated from panels a and b as a function of the vapor pressure. In the inset, the response curves of the uncoated ZnO and the response curve to ethanol of the porphyrins coated ZnO are magnified. (d) Comparison of the absolute value of the sensitivity of the uncoated ZnO under UV illumination and coated ZnO under white light. Because the sensor response is a dimensionless quantity, the unit of sensitivity is the inverse of partial pressure.

In the dark, the resistance of both coated and uncoated ZnO nanorods was not affected by the exposure to the VOCs. This behavior is expected for ZnO, where the gas sensitivity is enabled by either temperature or UV light. Porphyrins are sensitive to VOCs at room temperature; however, because no electron transfer takes place under dark conditions, any interaction occurring between the porphyrin and VOCs does not affect the conductivity of ZnO. Porphyrin sensitivity is then expected to be activated by the visible light. Figure 6 shows the resistance of uncoated ZnO nanorods (Figure 6a) and H<sub>2</sub>TPPCOOH-functionalized ZnO nanorods (Figure 6b) to the sequences of growing concentrations of ethanol and triethylamine, under UV lamp illumination for uncoated ZnO and white LED light illumination for H<sub>2</sub>TPPCOOH-functionalized ZnO. These results confirm that UV light activates the gas sensitivity of uncoated ZnO; in this case, as previously

discussed, the increase in the resistance in the presence of vapors is likely due to the consumption of photogenerated electron–hole pairs that are utilized in the reactions with the impinging volatile compounds.<sup>31</sup>

Photoactivation takes place also in H<sub>2</sub>TPPCOOH-functionalized ZnO nanorods. Noteworthy in this case, the activation is obtained with visible light, and, in particular, an appreciable sensitivity to triethylamine is found, whereas the response to ethanol is barely visible. (See the inset of Figure 6b.) The response to triethylamine is slowly reversible.

The sensing properties of photoactivated uncoated ZnO and H<sub>2</sub>TPPCOOH-coated ZnO are shown in Figure 6c. These Figures show the behavior of the sensor response versus the vapor partial pressure. The sensor response is evaluated as the relative change of resistance:  $(R_{\text{gas}} - R_{\text{air}})/R_{\text{air}}$ . The response of porphyrin-coated device illuminated by visible light to triethyl-

amine exceeds that observed in the other cases shown in Figure 6. A numerical estimation of the sensing properties is provided by the sensitivity, which is defined as the derivative of sensor response with respect to the vapor partial pressure.<sup>32</sup> A linear relationship between sensor response and concentration is assumed, and the calculated sensitivities are plotted in Figure 6d. For the sake of comparison, the absolute value of sensitivities is plotted on a logarithm scale. As evident from Figure 6c, the sensitivity of H<sub>2</sub>TPPCOOH-coated ZnO nanorods is negative, whereas the sensitivity of uncoated ZnO is positive.

Remarkably, the sensitivity to triethylamine is ~150 times larger than that toward ethanol, and such a sensitivity difference is rather unexpected for porphyrin-based gas sensors. As a comparison, previous studies reported that the ratio of sensitivity to triethylamine and ethanol of porphyrin-coated quartz microbalance and field effect transistor was found to be 1.5 and 16.5, respectively.<sup>33</sup>

It is worth reminding the transduction mechanism operating in quartz microbalances and field effect transistors: the first are sensitive to the variations of the absorbed mass and the second are sensitive to the surface potential.

For the sensor illustrated here the sensing mechanism is based on the electron transfer to the ZnO nanorods operated by the porphyrin-analyte adduct. Porphyrin layers can exploit a manifold of different interactions to bind ethanol and triethylamine, ranging from hydrogen bond to van der Waals forces. Because the sensitivities of porphyrin-coated quartz microbalance to triethylamine and ethanol are barely similar, as mentioned above, the amount of adsorbed ethanol molecules is comparable to the amount of adsorbed molecules of triethylamine. For this reason, the higher sensitivity observed in the case of triethylamine could be reasonably related to the better electron donor properties of the triethylamine than ethanol, which consequently induces a more efficient electron transfer process to the ZnO nanorods.

The invoked sensing mechanism for triethylamine is also consistent with the observed slow reversibility of the response to this vapor. Indeed, until the sensor is illuminated by visible light, the porphyrin–triethylamine complex is positively ionized onto the surface of ZnO. Then, even if the partial pressure of triethylamine in air drops to zero, there are no electrons available to restore the pristine triethylamine conditions. For this scope, it is necessary to remove the illumination to allow the excess of electrons in ZnO to recombine with the porphyrin–triethylamine complex, making possible the triethylamine desorption.

In the case of ethanol, because the interaction involves only a limited amount of electron transfer, the signal is promptly reversible, as observed in the inset of Figure 6b.

## CONCLUSIONS

The quest of materials for photovoltaic applications leads to the development of hybrid organic–inorganic assemblies that, besides being promising for light energy harvesting, are also characterized by enhanced additional properties. In this Article, the combination of porphyrins and ZnO nanorods has been investigated. Porphyrin-coated ZnO nanorods, grown in the gap region between two ITO electrodes, show remarkable photoconductivity properties in the visible region, where the spectral photocurrent recovers the absorbance spectrum of porphyrin. Furthermore, the gas sensitivity of the device is strongly driven by the sensing properties of the porphyrin and

more strikingly the exposure to visible light activates the sensitivity of the sensor.

Porphyrins have been widely used for many years as functional materials for chemical sensors in a number of applications from food quality to cancer diagnosis.<sup>34,35</sup> Their outstanding features are balanced by some restrictions in terms of transduction techniques. In particular, porphyrin layers are barely conductive, with the consequence that the fabrication of porphyrin-based chemiresistors, except in few cases, is not possible. In this Article, we have shown that ZnO not only offers this possibility also introduces further degrees of freedom (e.g., the color of the illumination light) for the design of alternative porphyrin-based sensor array. Remarkably, the photoconductivity of porphyrin-coated ZnO nanorods shows a large sensitivity to triethylamine with respect to ethanol. Although the porphyrin is a relatively low-selective material, the combination of porphyrins and ZnO transduces into electric signals only those interactions where an effective charge transfer between the adsorbed molecule and the porphyrin takes place. This opens an interesting opportunity to increase the selectivity of porphyrin-based sensors.

## AUTHOR INFORMATION

### Corresponding Author

\*E-mail: dinatale@uniroma2.it.

### Notes

The authors declare no competing financial interest.

## ACKNOWLEDGMENTS

WE thank the Italian MIUR (RP, PRIN2009 project 2009Z9ASCA\_004).

## REFERENCES

- (1) Hagfeldt, A.; Boschloo, G.; Sun, L.; Kloo, L.; Pettersson, H. *Chem. Rev.* **2010**, *110*, 6595.
- (2) Wan, Q.; Li, Q. H.; Chen, Y. J.; Wang, T. H.; He, X. L.; Li, J. P.; Lin, C. L. *Appl. Phys. Lett.* **2004**, *84*, 3654.
- (3) Johnson, J. C.; Yan, H. Q.; Schaller, R. D.; Haber, L. H.; Saykally, R. J.; Yang, P. D. *J. Phys. Chem. B* **2001**, *105*, 11387.
- (4) Arnold, M. S.; Avouris, P.; Pan, Z. W.; Wang, Z. L. *J. Phys. Chem. B* **2003**, *107*, 659.
- (5) Keis, K.; Vayssières, L.; Lindquist, S.-E.; Hagfeldt, A. *Nanostruct. Mater.* **1999**, *12*, 487.
- (6) Hu, Y.; Xu, C.; Zhang, Y.; Lin, L.; Snyder, R. L.; Wang, Z. L. *Adv. Mater.* **2011**, *23*, 4068.
- (7) Xu, S.; Wang, Z. L. *Nano Res.* **2011**, *4*, 1013.
- (8) Brunink, J.; Di Natale, C.; Bungaro, F.; Davide, F.; D'Amico, A.; Paolesse, R.; Boschi, T.; Faccio, M.; Ferri, G. *Anal. Chim. Acta* **1996**, *325*, 53.
- (9) Montmeat, P.; Madonia, S.; Pasquinet, E.; Hairault, L.; Gros, C.; Barbe, J.-M.; Guillard, R. *IEEE Sens. J.* **2005**, *5*, 610.
- (10) Rakow, N. A.; Suslick, K. S. *Nature* **2000**, *406*, 710.
- (11) Filippini, D.; Alimelli, A.; Di Natale, C.; Paolesse, R.; D'Amico, A.; Lundstrom, I. *Angew. Chem., Int. Ed.* **2006**, *45*, 3800.
- (12) Di Natale, C.; Paolesse, R.; D'Amico, A. *Sens. Actuators, B* **2007**, *121*, 238.
- (13) Penza, M.; Alvisi, M.; Rossi, R.; Serra, E.; Paolesse, R.; D'Amico, A.; Di Natale, C. *Nanotechnology* **2011**, *22*, 125502.
- (14) Nardis, S.; Monti, D.; Di Natale, C.; D'Amico, A.; Siciliano, P.; Forleo, A.; Epifani, M.; Taurino, A.; Rella, R.; Paolesse, R. *Sens. Actuators, B* **2004**, *103*, 339.
- (15) Belkova, G.; Zav'yakov, S.; Glagolev, N.; Solov'eva, A. *Russ. J. Phys. Chem.* **2010**, *84*, 129.
- (16) Zhao, Q.; Yu, M.; Xie, T.; Peng, L.; Wang, P.; Wang, D. *Nanotechnology* **2008**, *19*, 245706.

- (17) Li, X.; Cheng, Y.; Kang, S.; Mu, J. *J. Appl. Surf. Sci.* **2010**, *256*, 6705.
- (18) Tu, W.; Lei, J.; Wang, P.; Ju, H. *Chem.—Eur. J.* **2011**, *17*, 9440.
- (19) Rochford, J.; Chu, D.; Hagfeldt, A.; Galoppini, E. *J. Am. Chem. Soc.* **2007**, *129*, 4655.
- (20) Saarenpaa, H.; Sariola-Leikas, E.; Pyymaki Perros, A.; Kontio, J.; Efimov, A.; Hayashi, H.; Lipsanen, H.; Imahori, H.; Lemmetyinen, H.; Tkachenko, N. *J. Phys. Chem. C* **2012**, *116*, 2336.
- (21) Stefanelli, M.; Monti, D.; Van Axel Castelli, V.; Ercolani, G.; Venanzi, M.; Pomarico, G.; Paolesse, R. *J. Porphyrins Phthalocyanines* **2008**, *12*, 1279.
- (22) Greene, L. E.; Law, M.; Tan, D. H.; Montano, M.; Goldberger, J.; Somorjai, G.; Yang, P. *Nano Lett.* **2005**, *5*, 1231.
- (23) Liu, B.; Zeng, H. *C. J. Am. Chem. Soc.* **2003**, *125*, 4430.
- (24) Lee, S. W.; Cho, H. D.; Panin, G.; Kang, T. W. *Appl. Phys. Lett.* **2011**, *98*, 093110.
- (25) Jensen, R. A.; Van Ryswyk, H.; She, C.; Szarko, J. M.; Chen, L. X.; Hupp, J. T. *Langmuir* **2010**, *26*, 1401.
- (26) Yan, F.; Huang, L.; Zheng, J.; Huang, J.; Lin, Z.; Huang, F.; Wei, M. *Langmuir* **2010**, *26*, 7153.
- (27) Cohen, R.; Kronik, L.; Vilan, A.; Shanzer, A.; Cahen, D. *Adv. Mater.* **2000**, *12*, 33.
- (28) Paolesse, R.; Monti, D.; Nardis, S.; Di Natale, C. In *Handbook of Porphyrin Science*; Kadish, K. M., Smith, K. M., Guilard, R., Eds.; World Scientific: Singapore; 2011; Vol. 12, p 121.
- (29) Abraham, M. *Chem Soc. Rev.* **1993**, *73*.
- (30) Di Natale, C.; Paolesse, R.; Macagnano, A.; Nardis, S.; Martinelli, E.; Dalcanale, E.; Costa, M.; D'Amico, A. *J. Mater. Chem.* **2004**, *14*, 1281.
- (31) Gong, J.; Li, Y.; Chai, X.; Hu, Z.; Deng, Y. *J. Phys. Chem. C* **2010**, *114*, 1293.
- (32) D'Amico, A.; Di Natale, C. *IEEE Sens J.* **2001**, *1*, 183.
- (33) Di Natale, C.; Buchholz, K.; Martinelli, E.; Paolesse, R.; Pomarico, G.; D'Amico, A.; Lundström, I.; Lloyd-Spetz, A. *Sens. Actuators, B* **2009**, *135*, 560.
- (34) Eifler, J.; Martinelli, E.; Santonico, M.; Capuano, R.; Schild, D.; Di Natale, C. *PLoS ONE* **2011**, *6*, e21026.
- (35) Di Natale, C.; Macagnano, A.; Martinelli, E.; Paolesse, R.; D'Arcangelo, G.; Roscioni, C.; Finazzi-Agrò, A.; D'Amico, A. *Biosens. Bioelectron.* **2003**, *18*, 1209.